AIP | The Journal of Chemical Physics

Rotational tunneling in CH4 II: Disorder effects

Werner Press, Igor Krasnow, Michaela Zamponi, and Michael Prager

Citation: J. Chem. Phys. **135**, 224509 (2011); doi: 10.1063/1.3664726
View online: http://dx.doi.org/10.1063/1.3664726
View Table of Contents: http://jcp.aip.org/resource/1/JCPSA6/v135/i22
Published by the American Institute of Physics.

Rotational tunneling in CH_4 II: Disorder effects

Werner Press,[1,a)] Igor Krasnow,[1] Michaela Zamponi,[2,b)] and Michael Prager[2,c)]
[1]*Institut für Experimentelle und Angewandte Physik der Christian-Albrechts-Universität Kiel, Olshausenstr. 40, D-24098 Kiel, Germany*
[2]*Jülich Centre for Neutron Science, Forschungszentrum Jülich GmbH, Outstation at the Oak Ridge National Laboratory, PO Box 2008, 1 Bethel Valley Road, Oak Ridge, Tennessee 37831, USA*

(Received 10 May 2011; accepted 8 November 2011; published online 12 December 2011)

Transitions within the tunneling multiplet of CH_4 in phase II have been measured in an experiment at the backscattering instrument BASIS of the Neutron Source SNS. They all involve transitions from or to T-states. A statistical model is put forward which accounts for local departures from tetrahedral symmetry at the sites of ordered molecules. Different from previous work, in which discrete sets of overlap matrix elements have been studied, now large numbers of elements as well as the ensemble of T-states are considered. The observed neutron spectra can be explained rather well, all based on the pocket state formalism of A. Hüller [Phys. Rev. B **16**, 1844 (1977)]. A completely new result is the observation and simulation of transitions between T-states, which give rise to a double peaked feature close to the elastic position and which reflect the disorder in the system. CH_2D_2 molecules in the CH_4 matrix are largely responsible for the disorder and an interesting topic for their own sake. The simple model presented may lend itself to a broader application. © *2011 American Institute of Physics*. [doi:10.1063/1.3664726]

INTRODUCTION

Solid methane (CH_4), particularly in phase II, serves as a model example for rotational tunneling of three-dimensional rotators. Intensive research has been carried out, both experimental and theoretical, aiming at a good understanding of the tunneling in CH_4 II and also of the phenomenon of rotational tunneling of hydrogenous molecules in general.[1,2] Many of these phenomena are well understood, but there is also a considerable amount of open questions. They include the nature of the T-states at the ordered tetrahedral sites in phase II, the role of disorder, the excitation spectrum of partially deuterated methanes and many features of the excitation spectrum in the orientationally ordered phase III in general.

Studies of the latter were rendered difficult by the lack of knowledge of the structure of phase III. By now the orthorhombic structure of CD_4 III has been determined[3] - CD_4 III is isostructural with CH_4 III - and this has encouraged several new high resolution neutron scattering experiments. Quite recently the structure of the moderately high pressure phase A, which is claimed to be identical with phase IV, has been solved as well.[4] However, unlike that of CH_4 III,[5–8] its structure is too complicated for providing another test of theoretical models for rotational tunneling. A review on the high pressure phases of solid methane has been published earlier.[9] Recently, a lot of emphasis has been given to the structure and electrical conductivity of solid methane at extremely high pressure with the motivation of finding the transition to a metallic phase[10–12] (or eventually a decomposition of the molecules[9]). Indeed there are indications of a semiconducting phase at pressures above 2 GPa.

CH_4 II has become a model quantum system for rotational tunneling also because of the knowledge of its crystal structure (space group Fm3c[13]), with high symmetry at the molecular sites. The crystal structure (Fig. 1) can be described by an fcc centre-of-mass lattice and partial orientational order. 6 of 8 molecules are orientationally ordered, while the remaining 2 in the unit cell are orientationally disordered.[13,14] This rather peculiar structure was theoretically predicted with a mean-field model employing electrostatic octupole-octupole interactions between the molecules[14] and later confirmed experimentally.[13]

There was a double motivation for the present work which ultimately has lead to a more complete formulation of disorder effects on the experimentally observable ground state multiplet in CH_4 II. The new measurements with CH_2D_2 in CH_4, performed at the backscattering instrument BASIS[15] of the spallation neutron source SNS at the Oak Ridge National Laboratory, are done with high energy resolution in a wide dynamical range. They aimed at (1) the tunneling spectrum of CH_2D_2 in phase II and in addition to this at (2) a much more precise information on line widths and line shapes for CH_4 than was available before. As pure CH_2D_2 is in phase III at low temperatures, the method of using CH_4 II as a host for CH_2D_2 seems to be the only way to achieve the first of the two goals. The experiment was conducted in the same spirit as an earlier one with 15% CH_3D in CH_4 II:[16] however, with nominally only 7.3% the contribution of CH_2D_2 to the total incoherent scattering is less than 4% - making this a difficult experiment. By far the dominant scattering is from CH_4 II, perturbed by CH_2D_2 "impurity molecules."

[a)]Author to whom correspondence should be addressed. Electronic mail: werner_press@yahoo.de.
[b)]Present address: JCNS Outstation at FRM II, Lichtenbergstr.1, 85747 Garching, Germany.
[c)]Deceased (November 2008).

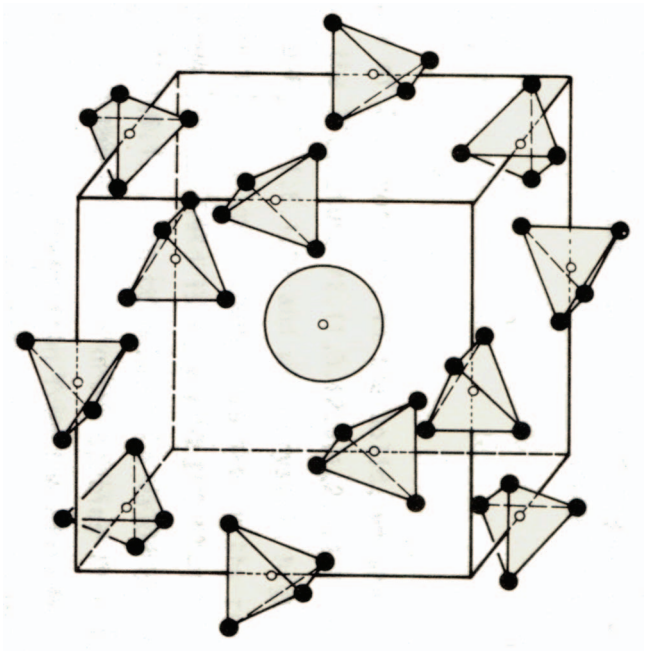

FIG. 1. Structure of CH_4 II; the surrounding of a disordered CH_4 molecule is shown.[13,14]

For an exhaustive analysis of the CH_2D_2 spectrum a rather precise description of the scattering from CH_4 II is needed. But there is considerably more to it. For many years there has been the question of finding the T to T (T-T) transitions within the ground-state multiplet of orientationally ordered methane molecules. The CH_4 peaks correspond to transitions between the rotational states related with the different spin species of symmetry A, T and E (with nuclear spin 2, 1 and 0). As disorder effects are always a part of rotational tunneling, the peaks have a considerable width even in the "pure" case.[17–19] In the present experiment the line widths and line shapes (full width at half maximum (FWHM) ~15% of the energy of the transition) are determined with higher precision than in all previous experiments. Then, for the first time - close to the elastic position and hence more or less hidden – the T-T contribution now has been found. In the course of this it is necessary to address the above questions related with disorder one more time. This also leads to a reconsideration of data from other methane samples, either with dilute guest molecules or solid solutions. One effect consists in modified effective octupole moments (see below), another, that molecules with smaller van der Waals radius (as well as vacancies) give rise to a local relaxation of the methane lattice. Both lead to modified potentials and rotational tunneling is very sensitive to such potential changes.

While a certain importance of accounting for an intrinsic disorder in the tunneling system has been stated before,[2,18,20] so far a more complete analysis has been missing. This will be given in the present paper, in which a simple disorder model is developed. The paper is organized as follows. We first give a brief summary both of some basic features of rotational tunneling and of the disorder effects characteristic for CH_4 II, with and without different molecules admixed. Then recent experimental observations at the neutron backscattering instrument BASIS are presented. This is followed by a first data analysis which is largely model-free but may serve for comparison with other data. In second theory part, existing approaches for the description of disorder effects are extended which allows one to fill in some of the existing gaps. The data analysis is accompanied by a detailed discussion of the T-states of CH_4 molecules and discussed within the model presented. Finally, a short outlook to other possible applications of the model is given and further work is briefly discussed.

THEORY I: ROTATIONAL TUNNELING IN CH_4 II

For a better understanding of the discussion a brief summary of some fundamental features of "rotational tunneling" will be presented. The molecular field at the ordered sites in CH_4 II is about 25 meV while the rotational constant of CH_4 is B = 0.665 meV. Therefore the molecular wave functions are well localized and written as products $\Psi = \Phi_\Gamma \chi_\Gamma$ of rotational wave functions Φ_Γ and nuclear spin functions χ_Γ; Γ denotes the symmetry (Γ = A, T and E). We do not distinguish between molecular $\overline{\Gamma}$ and site symmetry Γ, which is obligatory in certain cases.

As the spin of protons is 1/2, the total wave function must be totally anti symmetric with respect to a permutation of two hydrogen atoms. However, as only proper rotations corresponding to even permutations of hydrogen atoms are "feasible operations", the only requirement is that Ψ must be totally symmetric upon even permutations. Alfred Hüller has introduced the concept of pocket states,[1] narrow wave functions in the potential pockets. Corresponding to the 12 proper rotations of the tetrahedral group there are 12 such pocket states. They can be combined into a symmetric singlet A-state, three sets of triply degenerate T-states and a doubly degenerate E-state. Rotational states and spin states must have the same symmetry. This coupling has led to the introduction of the notion spin species, more familiar for H_2 molecules. In case of CH_4 the states can be equally labeled by the total nuclear spin of the molecules. The degeneracy of the A-state increases to 5 when including the nuclear spins.

Tunneling enters when the rotational wave functions overlap. Second order perturbation theory leads to the introduction of overlap matrix elements h and H, corresponding to 120° overlap and 180° overlap, respectively. For tunnel splittings of the order of 70 μeV and 140 μeV as in the case of CH_4 II, the 180° overlap can be neglected and then H = 0.[21] In this case the difference between the site symmetries $\bar{4}3m$ and $\bar{4}m2$, the latter is that of the "ordered" sites in phase II, can be ignored. The matrix H12 in Table C.1 (in Supplemental Material(C)[22]) represents the Hamiltonian matrix for general site symmetry. For tetrahedral site symmetry, that is all h_j equal, it has the energy eigenvalues $E_A = 8h$, $E_T = 0$ and $E_E = -4h$.

As shown by Hüller and Raich[21] a generalization to $E_A = 8h/(1 + 8\delta)$ and $E_E = -4h/(1 - 4\delta)$ is necessary in order to account for the overlap δ of the wave functions. For the ordered CH_4 molecules in CH_4 II the effect of δ on the observed transitions cannot be ignored.[18,19] The equivalent formulation for partially deuterated methanes is discussed in Ref. 16.

Transitions between the A and T states as well as the T and E states can be observed directly with inelastic neutron scattering while transitions between A and E are forbidden. The latter can be explained either (1) by symmetry arguments[2,23] or (2) by the conservation of the nuclear spin in the scattering process: a neutron can change the nuclear spin I of a CH_4 molecule by $+/-1$ only and hence no transitions from A ($I = 2$) to E ($I = 0$) with $\Delta I = 2$ are possible.[2,17]

Finally, transition matrix elements for neutron scattering can be calculated for the allowed transitions. The latter has been done using δ-functions as pocket states, which represents a considerable approximation. While associating the observed energy of transitions with a level scheme and symmetry allowed transition matrix elements (in case of general symmetry and possibly several crystallographically different sites) there is more information contained in the experimental data – the intensity and the line width of the peaks. In the case of tetrahedral symmetry the pocket state model yields an intensity ratio $I_{AT}/I_{TE} = 5/4$ for polycrystalline solid methane.[1] For more details concerning (coherent) rotational tunneling the reader is referred to, e.g., Refs. 1, 2, 21, and 24.

EXPERIMENT AND FIRST RESULTS

High resolution inelastic neutron scattering experiments have been performed at the backscattering silicon instrument BASIS of the Spallation Neutron Source SNS at the Oak Ridge National Laboratory. The instrument uses large analyzer banks with unpolished Si(111) crystals and has a Q-averaged resolution of 3.0 μeV. A series of experiments on partially deuterated methanes, namely solid CH_3D and CH_2D_2, both in their phase III, has been performed. A third experiment was devoted to CH_2D_2 "impurities" in CH_4 II with tetrahedral symmetry at the sites of ordered molecules.[13,14] It is only this latter experiment which will be discussed in the present paper. Matrix-isolated CH_2D_2 or CH_4 with CH_2D_2 "impurities" was obtained by co-condensing the two gases in a mixture with a nominal concentration of 7.3% CH_2D_2 prepared in the gas phase with a gas handling system as described in the supplemental material (A).[22]

Sample preparation and scattering experiment

The main constituent of the sample is normal hydrogenated methane. High purity CH_4 (99.995% purity) was used. The admixture, partially deuterated methane CH_2D_2, was supplied by Cambridge Isotope Laboratories, Andover, Mass., USA. The quoted chemical purity was 98% with the main impurity (about 2%) air. We also must assume that percent fractions of CH_3D and CD_3H are present, that is slightly less than 100% of the partially deuterated methane is CH_2D_2 (we guess ~95%; the scattering from the other constituents will not give rise to measurable peaks, particularly in the solid solution investigated). No further purification was performed, and no chemical analysis of the constituents nor of the solid solution was done.

The gases were condensed into a flat aluminum sample container with a nominal thickness of 0.1 mm. It was oriented at an angle of 45° with respect to the incoming neutron beam. The calculated transmission of the rotated cell filled with CH_4 is 85.5% in the high temperature limit. The observed complete conversion is caused by the paramagnetic oxygen molecules, admixed together with the CH_2D_2. The same phenomenon was noted for CH_3D in CH_4.[17] Due to this nuclear spin conversion the transmission decreases when lowering temperature. For a CH_4 sample at $T = 0$ K, fully converted to the A-state, the scattering doubles and the transmission decreases correspondingly. This also means that multiple scattering is temperature dependent. No multiple scattering corrections have been performed, however.

The measurements have been done in a temperature range of 1.9 K–20 K. The covered momentum transfer range is 0.2–2 $Å^{-1}$; the data were integrated into two Q-ranges with mean Q-values of 0.65 and 1.55 $Å^{-1}$. A separation into more "Q-bins" is possible at the cost of reduced counting statistics. In the present analysis, we have concentrated on spectroscopic features and hence on the data labeled with the Q-value 1.55 $Å^{-1}$. The data have been normalized to the monitor.

Background and resolution

Relatively short background scans were performed with the empty cell at a temperature of $T = 100$ K. Counting times were short as the cell contributes to only about 3% of the elastic intensity.

The instrumental resolution was measured with exactly the same geometry as used during the tunneling experiments. For this purpose the CH_3D sample was heated to a temperature of $T = 40$ K – this means to the orientationally disordered phase I which displays classical rotational diffusion of the molecules. There are no inelastic peaks but only a 2 meV wide ($T = 40$ K) "quasi elastic" scattering of Lorentzian shape. In the range of the experiment ($|\Delta E| \lesssim 200$ μeV) it provides an almost flat contribution to the background. A disadvantage of this way of measuring the resolution are very weak Bragg contributions from the 111-peak, when indexing within the fcc structure of phase I of CH_4. With a FWHM of 3.0 μeV (characteristic for plate geometry), the resolution is very good. As its shape is quite asymmetric the resolution was fitted with a sum of 5 Gaussians. This description of the resolution was used in the initial analysis. All initial fits of the data have been performed in DAVE, a program for data analysis.[25]

For the final fits with use of the algorithm accounting for orientational disorder a somewhat different approach was employed. After application of a careful smoothening procedure with use of spline methods the empty cell background was subtracted in the elastic range both from the resolution scan and the methane data. After the background subtraction the resolution also was smoothened with spline methods. The statistics of the empty cell scattering was too low for energy transfers >25 μeV for proceeding in the same way. This part of the background largely is caused by the sample itself. In the fits it was determined by using "fix points" little influenced by the tunneling peaks – obviously in the valleys outside the A-T and T-E transitions - and fitting it with polynomials of low order. For the data fits the least squares procedure (leastsq) from the PYTHON package SciPy was used.

Experimental results

Here our main interest is in the scattering from CH_4 II at low temperatures, both the inelastic peaks and the additional intensity close to the elastic position – with an elastic peak which is more than one order of magnitude stronger. The scattering from CH_2D_2 was included into the fits but will not be discussed here.

The data measured at T = 1.9 K are shown in Fig. 2(a) and display the combination of high resolution and excellent counting statistics obtained at BASIS. The measured spectrum is dominated by the peaks at energies +/− 74 μeV (E-T) and +/− 141 μeV (A-T). As expected, the peaks from CH_2D_2 are very weak, but observable. The presence of CH_2D_2 in the sample is also indicated by an additional broadening of the tunneling peaks of CH_4 II compared to pure CH_4 II. For comparison we also show data taken at the temperature T = 7 K (Fig. 2(b)). At T = 7 K the population differences in the ground state multiplet are small - the effect of detailed balance becomes visible. The analysis requires the introduction of relaxation processes. A discussion of this temperature dependence of the tunnelling in CH_4 is outside the scope of the present paper, however.

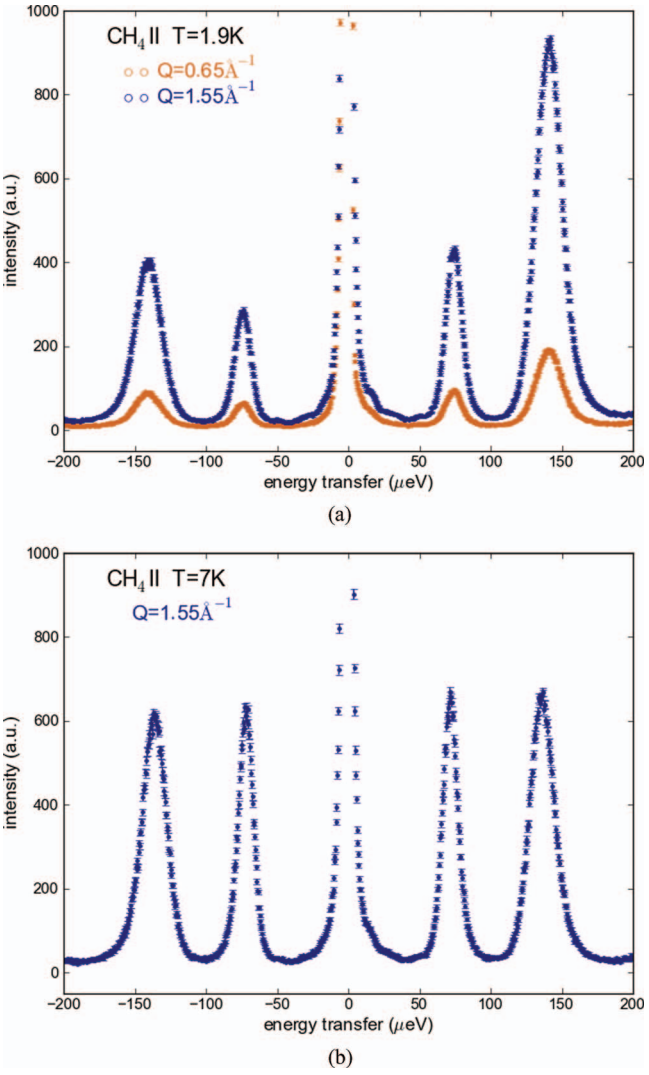

FIG. 2. CH_4:CH_2D_2(7.3%) II data: (a) Spectra taken at T = 1.90 K for average wavevector transfers Q = 0.65 Å^{-1} (brown) and Q = 1.55 Å^{-1} (blue). The intensity ratio between corresponding peaks in the 2 spectra is 4.2. The elastic intensity I_{el} rises to 25600 for Q = 1.55 Å^{-1}. (b) Spectrum at T = 7.0 K (Q = 1.55 Å^{-1}): it demonstrates the effect of the nuclear spin conversion and detailed balance as compared with the data from T = 1.9 K; I_{el} = 24200.

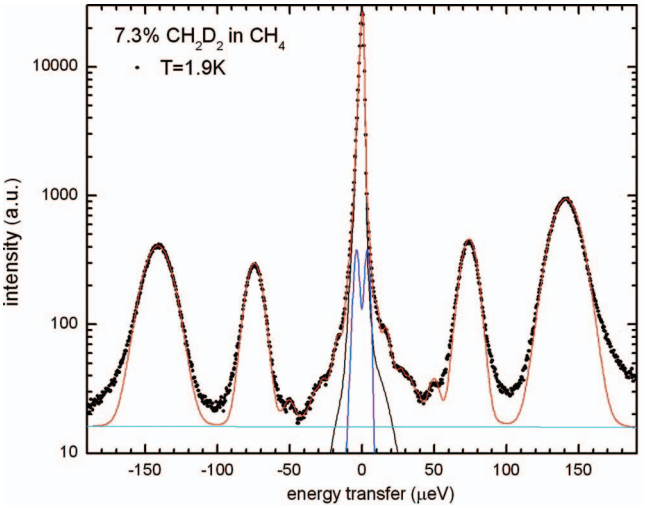

FIG. 3. Data with fit of CH_4:CH_2D_2(7.3%) II with a resolution of 3.0 μeV (black line) at T = 1.90 K. Fit results of all tunneling peaks are represented by the red line, the double peak in the centre is shown in blue and the background in light blue. The intensity is given in a logarithmic presentation in order to amplify the contributions of lower intensity - like that from CH_2D_2 II at energies 12.2, 30.6 and 52.8 μeV, respectively.

Data with fit results in a logarithmic presentation are shown in Fig. 3. The logarithmic intensity scale amplifies the contribution from ranges with low intensity, in particular those from CH_2D_2. In the fits Gaussians convoluted with the experimental resolution are used. For the tunneling peaks of CH_4 they yield the energies 74.2 and 141.1 μeV; the widths (FWHM) are 12.6 and 22.1 μeV, respectively. At present the CH_2D_2-contribution is included by 3 broad peaks at the appropriate energies, see Tables in Supplemental Material (B).[22] Their integrated inelastic scattering is roughly 4% of the total inelastic scattering. This matches with the nominal concentrations of the gases during the condensation. All 3 observed peaks could be envelopes of several transitions and it may be that there are unresolved transitions at lower energy – hidden by the "elastic peak".

There is yet another unresolved contribution - below the elastic peak. Initially it looked like a quasielastic contribution. But it turned out rather quickly that fitting this contribution with two Gaussian peaks centered at non-zero energies (about +/− 3 μeV) considerably improves the quality of the fit. The intensity of this part of the scattering is too strong for a contribution from CH_2D_2 – it must originate from CH_4. This immediately leads to suspect that it is related with T-T transitions. Both, position and intensity of this contribution have rather large uncertainty as these parameters are correlated with others describing features close to the elastic peak. All parameters obtained are given in the Tables B.1 and B.2 of Supplemental Material (B) together with other published results.[16,18,26,27]

In the following we concentrate on the tunneling of CH_4. The line positions are very close to those of CH_4 with

15% CH_3D: the perturbation of the CH_4 states by a CH_2D_2 molecule hence is roughly twice that of a CH_3D molecule. This matches with the increase of their effective octupole moments: for CH_2D_2 it is twice as large as for CH_3D. In addition there will be effects related with local displacements of the impurity molecules and the anisotropy of librational amplitudes of the CH_4 molecules themselves.

THEORY II

Disorder: Reported descriptions

Apparently, disorder aspects are an inseparable feature of tunneling in molecular solids. The disorder leads to a broadening of the tunneling lines which can be substantial and hence must be included in the description of tunneling data. In many cases a phenomenological approach has been used with a line width proportional to the energy transfer. While quite economical concerning the number of fit parameters needed, only in a few cases there is a basic justification for this procedure.

An alternative approach has been reported in Ref. 18, which is directly related with rotational potentials and the corresponding overlap matrix elements. It has been used for describing an experiment where particular care was taken in measuring energies, intensities and line widths of the A-T and T-E transitions within the ground-state multiplet of molecules at the ordered sites of CH_4 II[18,19] down to lowest temperatures.

The observed inhomogeneous broadening was associated with the existence of an "alloy" of different nuclear spin species. States with different symmetry Γ have different effective octupole moments and hence contribute differently to the rotational potential. A binomial distribution model describes the effects; for all details it is referred to Ref. 18: an important approximation of the model is that the local symmetry remains tetrahedral and therefore there is no splitting of the T-states. Nonetheless the simple "binomial" model was very successful in describing an experiment with an oxygen doped methane sample (to catalyze nuclear spin conversion) performed down to very low temperatures.[19]

Disorder: New approach

The suggested approach does not attempt to describe the disorder within the framework of orientation-dependent interactions and local potentials (expressed as a function of Euler angles or equivalently in terms of quaternions[29]). Rather, a local Hamiltonian matrix is introduced which can be separated into one with mean values for the overlap matrix elements and one with local departures from the (average) site symmetry $\bar{4}$m2,

$$\mathbf{H} = \langle \mathbf{H} \rangle + \delta \mathbf{H}, \tag{1}$$

where $\mathbf{H}$ is a 12×12 matrix connecting the 12 different pocket states, generated by the 12 proper rotations of a tetrahedron, as outlined above. The actual numbering of the pocket states (Figure C.1, also see Fig. 3 of 1) and the Hamiltonian matrix H12 for general symmetry (describing $\mathbf{H}$ and $\delta\mathbf{H}$) are given as Supplemental Material (C).[22] In the following the 180° overlap matrix elements are neglected.

In all previous experiments including "pure" CH_4[17–19,26] only the 2×2 "inelastic" tunneling peaks have been observed and discussed. Here, in addition to the disorder caused by the "alloy" of spin species there is an effect by the CH_2D_2 "impurities" which somewhat increases the disorder and hence the observed widths.

This latter contribution is of dynamical origin (see discussion in Ref. 28). Compared to CH_4 and, disregarding its different spin species, CH_2D_2 has an (i) enhanced octupole moment[26] (average molecule CX_4 with $m_X = 1.5m_H$ has a smaller librational amplitude) which needs to be included in a James-and-Keenan-like approach[14,20] and removes much of the compensation of terms in pure CH_4. In addition (ii) the librational amplitudes of the asymmetric top CH_2D_2-molecule around the 3 axes differ and (iii) the "classical" CH_2D_2-molecule has 6 possible orientations at each ordered site which give rise to 6 different centre-of-mass displacements of the molecular impurity and the corresponding modification of the interaction potential. These effects, however, do not change the reasoning. On the contrary, it may well be, that only the enhanced disorder due to the presence of CH_2D_2 impurities has rendered the experimental observation of the "T-state splitting" possible.

Diagonalisation of the 12×12 matrix H12 in general leads to 5 different eigenvalues, A, $3 \times$ (3 T) and (2 E) states. The further strategy is as follows: in order to simulate the *local* disorder N sets of transition matrix elements with a Gaussian distribution around $\mathbf{h}_0$ are generated, with N ranging between 10^4 and 10^6, corresponding to the needs. It has been shown[1] that for describing the T-states only, it is sufficient to use the 3×3 submatrix H_T of H12. In Eq. (2) h_4 always occurs with a positive sign and hence is distinguished in this presentation. D is the ground state energy,

$$\mathbf{H}_T = \begin{pmatrix} D & -h_1 - h_2 + h_3 + h_4 & -h_1 + h_2 - h_3 + h_4 \\ -h_1 - h_2 + h_3 + h_4 & D & h_1 - h_2 - h_3 + h_4 \\ -h_1 + h_2 - h_3 + h_4 & h_1 - h_2 - h_3 + h_4 & D \end{pmatrix}. \tag{2}$$

Starting from this submatrix eigenvalues and eigenvectors are calculated and used to determine the transition matrix elements for neutron scattering (Refs. 23 and 2), employing formulations for general symmetry. Here one has to select ei-

ther the spin-flip scattering or the non-spin-flip scattering in Table A.1 of Ref. 2. The results do not depend on the particular choice.

Disorder: T-state distribution and detailed model

An assumption must be made concerning the realization of the disorder. Initially we have assumed independent Gaussian distributions for all four 120° overlap matrix elements h_1,h_2, h_3 and h_4 or rather for δh_1,δh_2, δh_3 and δh_4 around a mean value $\mathbf{h} = (h_0, h_0, h_0, h_0)$ – all with the same variance $\eta \ll -h_0$. Here we have introduced 4D unit vectors **e.** From fits $h_0 \cong -17.9$ μeV and by comparison with the width of the A-T and T-E transitions $\eta \cong 1.8$ μeV (FWHM of the AT transition about 15%) is determined. While all the components of **h** must be negative, there is no restriction to the signs of the δh_j (j = 1 to 4).

In a way such a distribution leads to a density of T-states, and the spectrum of eigenvalues obtained with an isotropic distribution shows a 3-peak structure. This result was not expected, rather a single peak centered at E = 0 (note: the sum of the 3 eigenvalues of the 3×3 T-states is always zero).

The inclusion of disorder effects opens a completely new perspective regarding the T-states. The whole ensemble of T-states becomes visible - at least in principle: in previous discussions of different site symmetries, in particular of sites with symmetries 2 and 3, only discrete sets of **h** were considered.

Matrix elements h: d.o.s. and 4D-unit sphere

Of course, this density of states is not the observed quantity in the experiment. Instead, the observation is sort of a convolution of two different states mediated by the scattering of a neutron, that is, the transition matrix elements for neutron scattering get involved. Before actually doing this and describing observable and observed neutron spectra a closer inspection of the T-states is useful.

For this purpose coordinates on the 4D-unit sphere are introduced. The vector **h** also can be written as $\mathbf{h} = h(x_1, x_2, x_3, x_4) = h\mathbf{x}$, with h the modulus of **h** and the **x** coordinates on the 4-dimensional unit sphere ($\sum x_i^{\,2} = 1$) – that is the x_i also can be viewed as quaternions.[29] As in the chosen distribution (see Fig. 5) both the modulus h and the set of **x** change it seemed appropriate to investigate the "T-density of states" (d.o.s.) when varying only the angular or direction component **x** of **h.** For more background information it is referred to papers by A. Hüller *et al.*, e.g.,[1] no detailed discussion is given here.[30]

In practice the calculation of this d.o.s. has been done by generating a large set of (δ)**h** values ($N = 1\times10^6$) as random numbers in a 4D cube and projecting the values in the largest possible sphere inside the original cube onto its surface. The result is shown in Fig. 4 for h = 1: the d.o.s. is quite different from a Gaussian. It is symmetric and has a 3-peak structure with maxima at −2, 0 and +2 μeV, respectively. The peak at E = 0 is particularly pronounced (possibly due to a divergence), while those at ≈±2 μeV are more cusp-like – all related with the shape of the matrix H_T. Also there are symmetric cut-offs, a tribute to the restriction on the unit sphere.[31]

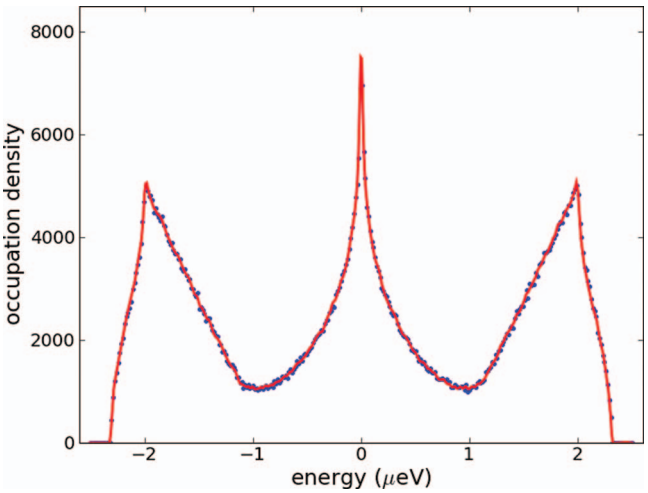

FIG. 4. Histogram with all allowed T-states on a 4-dimensional unit sphere; the red line represents a spline fit through the data, the blue points 1/3 of the data points of the original histogram obtained with about $3 \cdot 10^5$ sets of random numbers; there are 3 pronounced peaks at 0 and about ±2 μeV, respectively. Note that this is an occupation density of T-states and not yet represents transitions between T-states

Qualitatively the passage from |h| = 1 and the 4D unit sphere to a distribution of general **h** is performed in the following way: with the volume of a spherical shell in 4D space $S_3 dh = 2\pi^2 h^3 dh$ a weighting function $\sim h^3 \exp(-h^2/2\eta^2)$ multiplies the d.o.s. in Fig. 4. It has little effect on the peak at $E_T = 0$ μeV and both shifts and broadens the peaks at $E_T \approx \pm 2$ μeV. Transitions between the two outer peaks become washed out and are less visible. The energy position of the remaining two peaks can be estimated with the above reasoning to be at $2\sqrt{3}\eta$ which is larger than the simulated value of about 5 μeV. For anisotropic distributions ($\eta_A \neq \eta_T$, see below), the argumentation is less straightforward.

A frequently asked question has been whether the energy of any T-state E_T can exceed that of the E-state (E_E). This also can be settled numerically using transition matrix elements on the 4D unit sphere, but now restricted to the hexadecant with all signs negative. This is because transition matrix elements h_j must be negative. For approximately 5×10^5 sets of h_j the difference $E_E - E_T$ has been calculated and always is found to be >0; this means that E_E is always larger than E_T. Only for $\mathbf{h} = (-1, 0, 0, 0)$ and permutations, E_E and two of the eigenenergies E_T agree. This limiting case describes uniaxial rotation, - the same energies and degeneracies as for the uniaxial rotation of CH_3-groups or NH_3. Hence for 3D-rotation the E-level is always on top of the level scheme.

Symmetry-adapted coordinates and fits with general distributions

While some of the detailed features of the T-states are lost in the scattering process ("convolution" between T-states), a pronounced non-Gaussian signature remains, namely a double peak characteristic for the T-T transitions. Evidence of the double peak in the experiment requires a variance of the distribution sufficiently large compared to the experimental resolution. It is found, e.g., when taking a spherically symmetric distribution of $\boldsymbol{\delta}\mathbf{h}$ (with a single variance $\eta \sim 1.8$ μeV).

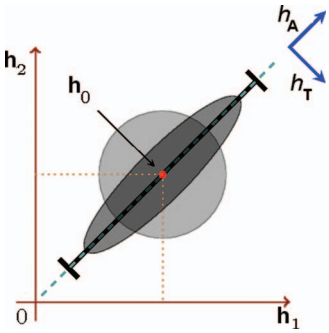

FIG. 5. Sketch of distributions in **h**-space in 2 dimensions highlighting 3 different situations with different shapes of the distribution: (i) circle: isotropic with $\eta_A = \eta_T$; (ii) ellipsoid: anisotropic with $\eta_A \neq \eta_T$; (iii) line: limiting case for $\eta_T = 0$ - equivalent to binomial distribution model

However, when using this "spherical model", the widths of the A-T and T-E transitions become very similar, while experimentally they are quite different.

This problem can be solved with introduction of orthonormal coordinates in the 4D-space of transition matrix elements $(\delta)\mathbf{h}$ different from the standard $\mathbf{e}_j$ (with $\mathbf{e}_1 = (1, 0, 0, 0)$, etc). Instead, **h** can be decomposed into a totally symmetric A-component and 3 T-components (see sketch in Fig. 5).

While the A-symmetric component only modulates the magnitude of the potential, those with T-symmetry reduce the symmetry of the potential (or that of the site). The corresponding unit vectors are as follows:

$$\begin{aligned} \mathbf{e}_A &= (1, 1, 1, 1)/2, \\ \mathbf{e}_{T1} &= (-1, -1, 1, 1)/2, \\ \mathbf{e}_{T2} &= (-1, 1, -1, 1)/2, \\ \mathbf{e}_{T3} &= (1, -1, -1, 1)/2. \end{aligned} \tag{3}$$

There are different conventions used for the numbering and the signs of the T coordinates which implicitly have been used by different authors. A particular set of **h** then can be decomposed into the above unit vectors as follows:

$$\begin{aligned} \mathbf{h}_A &= \mathbf{h} \cdot \mathbf{e}_A = (h_1 + h_2 + h_3 + h_4)/2, \\ \mathbf{h}_{T1} &= \mathbf{h} \cdot \mathbf{e}_{T1} = (-h_1 - h_2 + h_3 + h_4)/2 = u, \\ \mathbf{h}_{T2} &= \mathbf{h} \cdot \mathbf{e}_{T2} = (-h_1 + h_2 - h_3 + h_4)/2 = v, \\ \mathbf{h}_{T3} &= \mathbf{h} \cdot \mathbf{e}_{T3} = (h_1 - h_2 - h_3 + h_4)/2 = w. \end{aligned} \tag{4}$$

With these definitions the matrix $\mathbf{H}_T$ can be rewritten as

$$\mathbf{H}_T = \begin{pmatrix} D & 2u & 2v \\ 2u & D & 2w \\ 2v & 2w & D \end{pmatrix}. \tag{5}$$

In the following D = 0 will be used.

How does the model originally used by Heidemann *et al.*[18] fit into the above scheme? This latter model employs a binomial distribution of nearest neighbors (which is directly related with the magnitude of the potential) and completely remains within tetrahedral or A-symmetry. Only values $\mathbf{h} = h\mathbf{e}_A$ with h variable are allowed and obviously this does not give rise to T-state splittings ($\delta h_T = 0$). For splittings to occur different components of **h** must differ in magnitude: they must have non-zero components of T-symmetry, that is $\delta h_T \neq 0$.

The 3 possible cases for distributions of the transition matrix elements are sketched in Fig. 5. In agreement with the symmetry requirements at the tetrahedral site 2 different variances η_A and η_T are allowed. Similar symmetry requirements need to be respected for other site symmetries.

$\boldsymbol{\delta}\mathbf{h}_T$ apparently represents a "transverse" component of **h**, while δh_A is the dominant term contributing to the variation of the modulus of **h**. In the "binomial" model several discrete values of $\delta\mathbf{h}_A$ are the only allowed disorder effect and as a consequence of the A-symmetry only the magnitude of the **h** is modulated. As the instrumental resolution (in addition to other disorder effects) more or less removes the discrete characteristics of the binomial model, for $\delta h_T = 0$ the models are equivalent and the widths generated agree. In the presence of a transverse component the width η_A is somewhat smaller than that for $\eta_T = 0$ as the (small) effect of η_T on the modulus of h needs to be compensated.

The resulting parameters are $\eta_A = 2.3$ μeV and $\eta_T = 1.0$ μeV. This means that the disorder in CH_4 with CH_2D_2 has an ellipsoidal distribution (Fig. 5) - which leads to a sizable T-state splitting. The value of η_T must be related with the characteristics of the perturbation of the orientational order including the effect of the CH_2D_2 molecules. While there are qualitative arguments, a quantitative explanation based on interaction potentials[14,20] still needs to be given.

Neutron scattering: Transition matrix elements

The computer program was written with particular emphasis on the calculation of neutron spectra based on 10^4 or more sets of transition matrix elements **h.** At the same time most of the old calculations and conclusions were revisited. A central part of this computer program is the matrix A.1 of Refs. 2 and 23 which needs to be rotated following the algorithm outlined in these references (see Ref. 30). More specifically, the rotation concerns the 9 × 9 submatrix of A.1 of Ref. 2 which describes the transitions between the T-states. There are a few aspects which still need to be discussed:

1 The starting point of the description are the orientationally ordered sites of CH_4 II with symmetry $\bar{4}$m2. With the distributions discussed above disorder is introduced into the concept. One now may argue that a small departure from high symmetry, that is from $\mathbf{h} = h_0(1,1,1,1)$, should lead only to small changes of the derived quantities. As regards the energy eigenvalues the perturbation is small indeed. This is different for the neutron scattering intensities within the T-state multiplet. Here the rotation matrix **R** enters which diagonalises the matrix $\mathbf{H}_T$. **R** only depends on the direction of u,v,w (the components of $\boldsymbol{\delta}\mathbf{h}$ along the 3 unit vectors $\mathbf{e}_T$) that is on $(u,v,w)/\sqrt{(u^2 + v^2 + w^2)}$ whence infinitesimal departures from the symmetric case have the same effect as large ones.
2 Strictly speaking the powder averaged intensity calculated for the A- symmetric case (unperturbed symmetry $\bar{4}$m2) has little meaning beyond the contribution to the

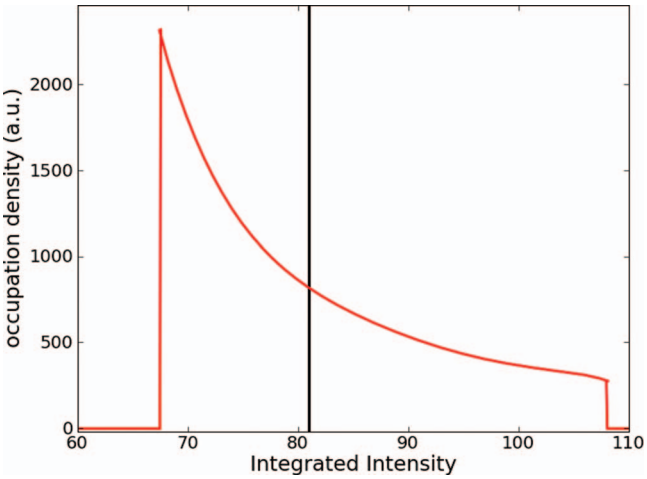

FIG. 6. T-T Intensity distribution for all **h** on the 4D unit sphere, calculated for an isotropic distribution for $N = 2.5 \cdot 10^6$ values of **h**. The average value of the integrated intensity is $y = 81$ (corresponding to an inelastic intensity 81-81 $j_0(Q\rho\sqrt{8/3})$. Again spline procedures have been used for smoothening the results.

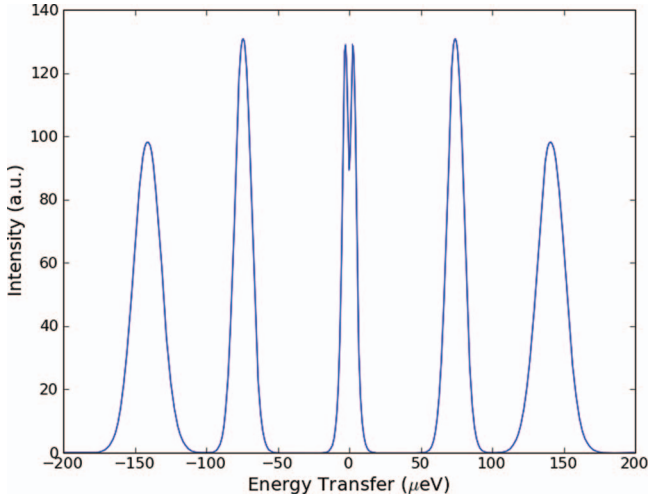

FIG. 7. Shape of CH_4 inelastic tunnelling transition modelled in the way described in the paper ($N = 10^6$ sets of overlap matrix elements). Gaussians are used for the resolution function in order to obtain symmetric peaks. In addition to the well-known inelastic peaks there is an obvious splitting of the T-T contribution in the centre.

total scattering of a CH_4 molecule from T-T transitions which is an invariant (high temperature limit; given in units of $\sigma_{inc}/216$, already used in the Tables in Refs. 2 and 23; this invariant is $81(3 + j_0(Q\rho\sqrt{8/3})$, where j_0 is a spherical Bessel function and $\rho = 1.093$ Å the C-H distance), as all T-T contributions are elastic in this case.

A numerical analysis based on the disorder models allows to separate elastic and inelastic scattering. The inelastic part of the T-T intensity is obtained by summing over the powder-averaged contributions from all 6 transitions between T-states with different energy. Different (and non-equivalent) directions ~ (u,v,w) give rise to different T-T intensities. This is depicted in Fig. 6. Here the frequency of occurrence of T-T intensities is shown.

The calculated histogram obviously is not symmetric. Both an isotropic distribution and also the more general anisotropic distribution introduced above lead to the same integrated T-T intensity of $y = 81$ in $y \cdot (1 - j_0(Q\rho\sqrt{8/3}))$. That is, the integrated inelastic T-T intensity centered at $\hbar\omega = 0$ (both up- and down scattering added) is predicted to have 3/5 of the A-T intensity and 3/4 of the T-E intensity (always reference to a single peak and all values are taken in the high temperature limit). The result is different from that previously reported /19/ which was taken from the special case of 3-fold symmetry. In any case, the calculated T- T intensity is relatively low.

Results obtained with the refined description

The CH_4 tunneling peaks of CH_4:CH_2D_2 have been fitted with the model described above. A single fit with $N = 2.5 \times 10^4$ sets of transition matrix elements (needed for sufficient statistical accuracy in the final fits) and with about 10–15 parameters takes about 5–10 h on a standard pc. This is rather slow, but fast enough for our purpose. Trends can be detected with much smaller numbers N. For reaching higher speed and shorter turnaround times one has to improve the algorithm used or use more powerful computers.

Before proceeding to the actual fit results the inelastic scattering from CH_4, shown in an idealized form in Fig. 7, is discussed. For reasons of clarity several simplifications have been used. A Gaussian resolution was taken in order to avoid an asymmetric shape of the T-T contribution as in the fits of the data. While the fit results have been used for most parameters (e.g., the width of the Gaussian distributions of δh_A and δh_T), the intensities taken are the theoretical values (high-T limit). The fitted intensity of the T-E contribution is only 2/3 of the theoretical value. Also, further refinements as described below have not been included in this presentation. The figure demonstrates the splitting of the T-T contribution as well as the widths of all contributions in a pure form. The lineshape of the T-T contribution is different from that of a sum of 2 Gaussians. Depending on the parameters of the distribution there may even be the indication of another double peak. As can be seen below the fits with spectra calculated on the basis of the disorder model are quite satisfactory: this concerns both the unresolved T-T transition and the resolved tunneling lines.

Figure 8 shows the data together with the fit. The main fit parameters concerning both CH_4 and CH_2D_2 are summarized in Table I. As before the CH_2D_2-contribution is included in the conventional fashion by 3 broad Gaussian peaks at the appropriate energies. Their positions remain largely unchanged compared to the initial "conventional" fits. All CH_2D_2-peaks now have a width of about 10 μeV (FWHM); their intensities change somewhat. Different from our expectation no additional information could be obtained, neither in the region of the elastic peak nor elsewhere. Apparently, the total scattering from CH_2D_2 is quite weak and due to the strong contribution from CH_4 there are correlations between the respective parameters. Though the present results will provide a good starting point for the interpretation of tunneling in CH_2D_2, ultimately it will be necessary to fit the 2 models (CH_4 II and CH_2D_2 II) simultaneously.

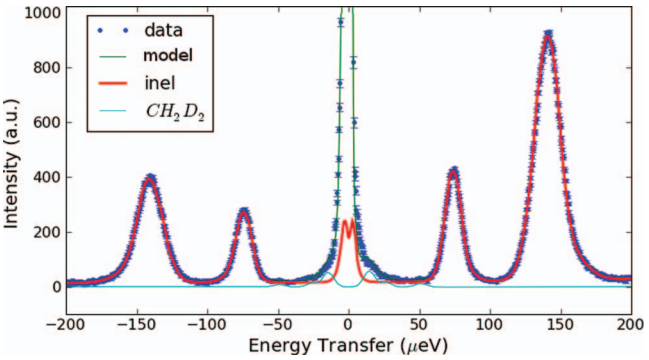

FIG. 8. Scattering from CH_4:CH_2D_2 at T = 1.9 K. Fit to the data with the disorder model described in the text (N = 25000). In addition the effect of a contamination with 0.3% air has been included into the fit.

Energies and eigenvalues of the T-states do not depend on the average transition matrix element h_0 but entirely on δh_T and δh_A, on δh_A the less the smaller δh_T. The shape of the T-T transition varies considerably with the particular distribution and the resolution. The newly observed contribution has an overall FWHM of about 10 μeV and indeed some similarity with a double peak represented by 2 Gaussians. The fit values $\eta_T = 1.07$ μeV and $\eta_A = 2.25$ μeV yield a splitting into a double peak (Fig. 8) with maxima at ± 2.7 μeV. With the present resolution the T-T transition is not fully resolved.

The fit parameter η_T has a somewhat larger uncertainty than the value for η_A. The information on their ratio is not only contained in the unresolved contribution to the elastic peak but also in the width of the A-T and T-E transitions. In the fits the simulated tunneling peaks were multiplied with temperature factors and 2 additional factors allowing for departures from the calculated intensities entirely based on the model. On a relative scale the uncorrected intensities are 5 for A-T, 4 for T-E and 3 when integrating all T-T contributions. The theoretical value of the ratio $R_2 = I_{AT}/I_{TT}$ is very well reproduced by the fits. While this good agreement may be fortuitous we believe that at least the right order of magnitude for the T-T scattering is confirmed.

TABLE I. Main fit results (a) obtained with the disorder model for CH_4 II and (b) fitting Gaussian peaks for the CH_2D_2 contribution: (a) h_0 is the average 120° overlap matrix element, η_A and η_T are the variances of the anisotropic distribution, δ is the overlap, $R = I_{AT}/I_{TE}$ and $R_2 = I_{AT}/I_{TT}$ are the intensity ratios discussed in the text: P_{air} denotes the fitted percentage of air molecules in the sample and Δh_0 the change of the 120° overlap at sites with a missing ordered CH_4 neighbor. Positions, FWHM = 2Γ and intensities of the contribution from CH_2D_2 are given in (b).

	(b)		
(a)	E(μeV)	2Γ(μeV)	Int (a.u.)
$h_0 = -18{,}20$ μeV			
$\eta_A = 2.25$ μeV	14.4	8.4	330
$\eta_T = 1.07$ μeV	28.4	12.2	170
$\delta = 0.0043$	53.0	10.6	90
$R = 1.49 = (5/4)1.19$			
$R_2 = 1.78 = (5/3)1.07$			
$P_{air} = 0.29\%$			
$\Delta h_0 = -2.9$ μeV			

On the other hand, the intensity ratio $R = I_{AT}/I_{TE} = 1.49$, which is 20% larger than the calculated value of 5/4, is the same as that found before. Experimentally determined intensity ratios apparently depend on details of the disorder (see table B.1 in suppl. material[22]). An extension from δ-type pocket states to states with finite and anisotropic width seems necessary.[23]

To obtain the quality of fit as displayed in Fig. 8 further steps of refinement were done and need to be reported: in all scans (including those at T = 1.9 K) detailed balance is found to reflect the actual temperature of our sample. This is due to nuclear spin conversion, caused by the presence of oxygen. We know that the leading impurity in CH_2D_2 is air which contains 20% of the paramagnetic molecule O_2. While completely different regarding spin conversion, N_2 and O_2 have very similar effects on the methane spectrum. These molecules are built into the lattice as substitutional impurities. In the dilute limit each of them affects its surrounding in the following way:

i Their nearest CH_4 neighbors are lacking 1 of 8 methane neighbors with its octupole moment: the potential they experience is much weaker which gives rise to weak and broad peaks shifted to higher energies.[19,27] An indication of such peaks indeed is present on the high energy side of the four tunneling peaks. From the fits we also get a rough idea about the amount of air in the sample. Each impurity molecule affects the excitation spectrum of eight methane neighbors. 2.5% of the molecules affected corresponds to ≈ 0.3% air (and hence 0.06% O_2) in the sample which corresponds to about 4% air in the CH_2D_2 gas. As there is considerable uncertainty in this result - the inelastic contribution is not well-separated from the main peak - we may take this value as an upper limit.

ii When referring to the A -T part of this small contribution its energy is centered at E = 172 μeV which corresponds to ∼60% of the calculated shift (and the shift of the corresponding energy found for CH_4:Kr, 194 μeV[27]). The reduction of this shift can be related with the small van der Waals radii of N_2 and O_2. They are considerably smaller than that of CH_4 which leads to a local lattice relaxation. In the first neighbor shell of a N_2 or O_2 molecule the CH_4 molecules are displaced in the direction towards the "defect". Locally there are smaller distances and hence an increase of the interaction potential occurs, which partially compensates the effect of the missing neighbor.

A final remark concerns the ratio between the energies of A-T and T-E transitions (see Theory I) which is markedly <2. The 180° overlap matrix elements H cannot be responsible as they are one to two orders of magnitude too small to yield the observed effect.[21] Rather, the overlap of the wavefunctions δ needs to be considered which enters into the expression for the transition energies, e.g., $\hbar\omega_{AT} = 8h/(1 + 8\delta)$. The ratio of the energies then is $r = [8h/(1 + 8\delta)]/[(1 - 4\delta)/h] \approx 2(1 - 12\delta)$. In the fit routine all A-T and T-E transitions have

been corrected by the respective factors which yields a value $\delta = 0.0043$ in close agreement with the value found by A. Heidemann *et al.*[18]

With decreasing potential both the overlap matrix elements and the overlap must increase. Therefore we have attempted to extract an h-dependent δ from the low temperature data for CH_4 with oxygen impurities.[19] As, however, the uncertainty of the reported energies was too high for the present purpose, a linear dependence $\delta(h) = 2.3 \cdot 10^{-4}$ h was assumed. The same assumption with a slightly different constant already has been used for estimating overlaps $h(H_2D)$ for CH_3D in CH_4 II.[16] There is only a limited effect on the fit results.

SUMMARY AND OUTLOOK

As has been stated above, disorder seems to be inseparable from rotational tunneling: in all known examples[32] a broadening of the tunneling peaks has been observed even at He-temperatures and below. For this reason it is important to include disorder into the analysis.

In this paper, we indicate a more refined way of describing disorder which is not only useful for CH_4 II. The microscopic origin of the disorder for several impurity atoms or molecules will be studied in a separate paper. For CH_4 II the attention has been drawn to the orientationally ordered molecules and the distribution of the T-states which are found to have considerable internal structure. There is also an effect on the rotational states of the orientationally disordered molecules in CH_4 II as well, but it is much less pronounced. An algorithm is presented in which local disorder around any chosen orientationally ordered CH_4 molecule in the crystal is introduced. This is done by first decomposing **h** into components with A- and T-symmetry. Distributions of **h** with general symmetry are assumed which, however, respect tetrahedral symmetry on average. Then, based on the pocket state formalism of A. Hüller,[1] energies and neutron scattering intensities for a large set of different transition matrix elements are calculated, again for general symmetry. Indeed an anisotropic distribution of overlap matrix elements h_j turns out necessary, with a distinction between "longitudinal" and "transverse" variances, η_{II} and $\eta_{\perp}$, or, in a stricter formulation, variances with A- and T-symmetry.

An experiment performed at the backscattering instrument BASIS at the SNS showed strong intensity below the elastic peak which is reasonably well described by a double peak. Obviously, the combination of high energy resolution and a large dynamical range (at high intensity) opens many new possibilities. While the uncertainty of the fit parameters remains fairly large the multi-peak structure is confirmed by the model and the fit parameters generalize previous findings based on a simpler model. A re-examination of the elastic region by employing higher resolution, e.g., backscattering at a reactor-based instrument with a resolution of about 1 μeV, looks promising, however.

The observed intensity of this contribution agrees very well with the calculations. An improved refinement was obtained by allowing for contributions (which may be called a "fingerprint" of N_2 and O_2 in CH_4) triggered by the presence of small amounts of air in the sample. Also, a very precise value for the (average) overlap δ of the wave functions which enters the normalization of the energies[17,21,33] was determined. As there is a direct relation between potentials V and energy eigenvalues E, potential and energy fluctuations ΔV and ΔE, respectively, are related as well ($\Delta V/V \approx 0.3 \cdot \Delta E/E$ in the relevant range of potentials[33]) which yields important additional information.

The above algorithm may replace the more simplistic assumption that the line width increases proportional to the energy of the transition (which, e.g., was successful in special case of NH_4ClO_4[34]). It also explains why the binomial distribution model[18] worked relatively well at least as far as the inelastic tunneling transitions are concerned.

As long as the site symmetry is high and the splittings are in the tunneling regime (with energies $\lesssim$10–15% of the rotational constant B) the application is straightforward for molecules with full tetrahedral symmetry (CH_4, CD_4, NH_4^+, ND_4^+). For lower site symmetry and multi site systems the required number of parameters will increase and render the approach more difficult to use. In the case of XD_4 the intensity ratios of the inelastic contributions (tetrahedral site symmetry) are I_{AT}:I_{TE}:I_{TT} = 5:6:7, instead of 5:4:3 for CH_4. Consequently, in relative terms, T-T transitions become more intense in XD_4.

A generalization to the partially deuterated tetrahedral molecules $XH_{4-y}D_y$ (X = C, N, y = 1, 2, 3) seems obvious. As in all previous cases the algorithm requires a formulation for general site symmetry which is non-trivial. The paper by Lushington, Maki *et al.*[28] gives by far the most complete description of the rotational states of partially deuterated methanes: beyond the need of introducing different tunneling matrix elements h_i for a lighter and a heavier group, molecular localization has to be introduced (as in general orientational potentials differ for different orientations).

Localization in conjunction with disorder, which may render the observation of the excitation spectrum with neutrons impossible, also plays a role for hydrogen in metals systems.[35,36] Tunneling of H in metals indeed is a possible application of the model to systems outside molecular ones. Also, for simpler tunneling systems like methyl groups (several potential parameters may be important) or H_2, an inclusion of disorder effects may yield interesting results.

The central limit theorem requires that the superposition of several disorder or resolution effects ultimately always leads to Gaussian distributions. This is also the case here and even "dramatic" effects like missing CH_4 molecules (N_2 and O_2 as substitutional impurities) are barely visible as peaks. The double peak originating from T-T transitions remains, however. More effects can be assigned to a microscopic origin for less pronounced disorder as CH_4 II with O_2 (with low oxygen concentration) at low temperatures.[19]

Furthermore there is still the need of a discussion of the scattering from CH_2D_2 in phase II which was part of the motivation of the present experiment. In this case, center-of-mass displacements of the molecules will modify local potentials substantially and must be taken into account. Centre-of-mass displacements play an even more important role in phase III of solid methane. Some new work on rotational tunneling

in phase III of CH_4 – analyzed with the knowledge of the phase III structure - already has been published.[8,37] For the partially deuterated methanes new data from IN16 at the ILL, Grenoble and BASIS at the SNS, Oak Ridge are available. It remains to be seen whether it will be necessary to proceed to rotation-translation coupling and solve a rotational Hamiltonian with inclusion of translational degrees of freedom or whether a more simplistic approach will suffice. The former has been done with great success by P. Schiebel *et al.* for uniaxial rotation.[38] A generalization to the rotational states in methane hydrate has recently been published by I. Matanovic *et al.*[39] and is more complicated.

ACKNOWLEDGMENTS

A portion of this research at Oak Ridge National Laboratory's Spallation Neutron Source was sponsored by the Scientific User Facilities Division, Office of Basic Energy Sciences, U. S. Department of Energy. Also in the name of M.P., W.P. wishes to thank the Oak Ridge National Laboratory and the members of the BASIS team for the warm welcome and support. One of us (WP) is thankful to the Institut für Experimentelle und Angewandte Physik at the University of Kiel for financial support of the measurement at SNS. We would like to thank A. Heidemann and K. Maki for helpful discussions and comments.

[1] A. Hüller, Phys. Rev. B **16**, 1844 (1977).
[2] W. Press, "Single Particle Rotations" in *Tracts of Modern Physics* (Springer, New York, 1981), and references therein.
[3] M. A. Neumann, W. Press, C. Nöldeke, B. Asmussen, M. Prager, and M. Ibbersen, J. Chem. Phys. **119**, 1586 (2003).
[4] H. E. Maynard-Casely, C. L. Bull, M. Guthrie, I. Loa, M. I. McMahon, E. Gregoryanz, R. J. Nelmes, and J. S. Loveday, J. Chem. Phys. **133**, 064504 (2010).
[5] M. Prager, W. Press, A. Heidemann, and C. Vettier, J. Chem. Phys. **77**, 2577 (1981).
[6] F. Lostak, K. O. Prins, and N. J. Trappeniers, Physica **B159**, 249 (1989).
[7] A. J. Nijman and N. J. Trappeniers, Physica **95B**, 147 (1978); A. J. Nijman, M. Sprik, and N. J. Trappeniers, *ibid.* **98B**, 247 (1980).
[8] A. Hüller, M. Prager, W. Press, and T. Seydel, J. Chem. Phys. **128**, 34503 (2008).
[9] R. Bini and G. Pratesi, Phys. Rev. B **55**, 14800 (1997).
[10] L. Sun, A. L. Ruoff, C.-S. Zha, and G. Stupian, J. Phys. Chem. Solid **67**, 2603 (2006).
[11] L. Sun, W. Yi, L. Wang, J. Shu, S. Sinogeikin, Y. Meng, G. Shen, L. Bai, Y. Li, J. Liu, H. Mao, and W. L. Mao, Chem. Phys. Lett. **473**, 72 (2009).
[12] H. Hirai, K. Konagai, T. Kawamura, Y. Yamamoto, and T. Yagi, Chem. Phys. Lett. **454**, 212 (2008).
[13] W. Press, J. Chem. Phys. **56**, 2597 (1972).
[14] H. M. James and T. A. Keenan, J. Chem. Phys. **31**, 12 (1959).
[15] E. Mamontov, M. Zamponi, S. Hammons, W. S. Keener, M. Hagen, and K. W. Herwig, Neutron News **19**, 22 (2008).
[16] K. J. Lushington, J. A. Morrison, K. Maki, A. Heidemann, and W. Press, J. Chem. Phys. **76**, 383 (1983).
[17] W. Press and A. Kollmar, Sol. State Comm. **17**, 405 (1975).
[18] A. Heidemann, W. Press, K. Lushington, and J. Morrison, J. Chem. Phys. **75**, 4003 (1981).
[19] A. Heidemann, K. J. Lushington, J. A. Morrison, K. Neumaier, and W. Press J. Chem. Phys. **81**, 5799 (1984).
[20] T. Yamamoto, Y. Kataoka, and K. Okada, J. Chem. Phys. **66**, 2701 (1977).
[21] A. Hüller and J. Raich, J. Chem. Phys. **71**, 3851 (1979).
[22] See supplemental material at http://dx.doi.org/10.1063/1.3664726 for (A) sample preparation, (B) parameters obtained from fits with Gaussians, (C) proper rotations of tetrahedron and Hamiltonian matrix H12 for general symmetry.
[23] A. Hüller and W. Press, Phys. Rev. B **24**, 17 (1981).
[24] Y. Ozaki, Y. Kataoka, and T. Yamamoto, J. Chem. Phys. **73**, 3442 (1980).
[25] R. T. Azuah, L. R. Kneller, Y. Qiu, P. L. W. Tregenna-Piggott, C. M. Brown, J. R. D. Copley, and R. M. Dimeo, J. Res. Natl. Inst. Stan. Technol. **114**, 341 (2009).
[26] M. Prager and W. Press, J. Chem. Phys. **92**, 5517 (1990).
[27] S. Grondey, M. Prager, and W. Press, J. Chem. Phys. **86**, 6465 (1987) and S. Grondey, PhD dissertation, Jül-Report 2083 (1986).
[28] K. J. Lushington, K. Maki, J. A. Morrison, A. Heidemann, and W. Press, J. Chem. Phys. **75**, 4010 (1981).
[29] W. R. Hamilton, Lectures on Quaternions (Hodges and Smith, Dublin 1835), http://en.wikipedia.org/wiki/Quaternion.
[30] The discussion of eventual singularities of the distribution of eigenvalues is not finished and possibly requires the use of spherical trigonometry in 4D; a qualitative discussion of matrix-properties points at singularities at the positions of the peaks at $E = 0\ \mu$eV and, possibly and less well understood, at $E \approx +/- 2\ \mu$eV.
[31] There is a misprint in Table A.1 in Ref. 2: rather than c_x, the 41 elements 7,12 and 12,7 of the matrix must read e_x (transition from E to T_x and vice versa, both with spin 0). Considerable care must be taken to keep the sequence of pocket states used for calculating the Table A.1 in Ref. 2.
[32] M. Prager and A. Heidemann, Chem. Rev. **97**, 2933 (1997).
[33] G. Voll and A. Hüller, Can. J. Chem. **66**, 925 (1988).
[34] M. Prager, W. Press, B. Alefeld, and A. Hüller, J. Chem. Phys. **67**, 5126 (1977).
[35] C. Morkel, H. Wipf, and K. Neumaier, Phys. Rev. Lett. **40**, 947 (1978).
[36] Canneli, R. Cantelli, F. Cordero, and F. Trequattrini, Phys. Rev. **49**, 15040 (1994).
[37] M. Prager, W. Press, B. Asmussen, and J. Combet, J. Chem. Phys. **117**, 5821 (2002).
[38] P. Schiebel and W. Prandl, Z. Phys. **104**, 137 (1997).
[39] I. Matanovic, M. Yu, J. W. Moskowitz, J. Eckert, and Z. Bacic, J. Chem. Phys. **131**, 224308 (2009).